Journal of Applied Polymer Science

Polypropylene reinforced with nanocrystalline cellulose: Coupling agent optimization

Hojjat Mahi Hassanabadi,[1] Ayse Alemdar,[2] Denis Rodrigue[1]

[1]Department of Chemical Engineering and CERMA, 1065 Avenue de la Médecine, Université Laval, Quebec, Quebec G1V 0A6, Canada

[2]FP Innovations, 2665 East Mall, Vancouver, British Columbia V6T 1Z4, Canada

Correspondence to: D. Rodrigue (E-mail: Denis.Rodrigue@gch.ulaval.ca)

ABSTRACT: Five different grades of maleic anhydride polypropylene (MAPP) having different molecular weight and acid value (AV) were used as coupler in PP-nanocrystalline cellulose (NCC) composites. The main objective was to study the effect of MAPP structure (Mw, AV) and filler/coupler (*F*/*C*) ratio on mechanical properties in order to find optimum mechanical properties in tension, flexion, and impact. Results showed that both Mw and AV have direct effect on mechanical properties and a balance between both must be achieved to get the best performance. However, regardless of MAPP structure, optimum improvement was obtained for $F/C = 7.5/1$. Shear rheological data showed that at high MAPP content, MAPP acts as lubricant. DSC and AFM analysis showed small reduction in the size of PP crystals in the presence of NCC. Rheological data under large amplitude oscillatory shear showed that the nanocomposites used here are under percolation. Using these analyses, possible reinforcement mechanisms were investigated. © 2015 Wiley Periodicals, Inc. J. Appl. Polym. Sci. **2015**, *132*, 42438.

KEYWORDS: cellulose and other wood products; composites; mechanical properties; nanoparticles; nanowires and nanocrystals

Received 17 October 2014; accepted 30 April 2015

DOI: 10.1002/app.42438

INTRODUCTION

Nanocrystalline cellulose (NCC), which is obtained by acid hydrolysis of cellulosic fibers, has been found to be a good candidate to improve the mechanical properties of polymeric systems.[1] Considering its inherent renewability and its relative availability, NCC has been the focus of several academic and industrial studies since its discovery.[1–3] However, a great challenge regarding its use in the plastics industry is the fact that most resins, such as polyethylene (PE) and polypropylene (PP), are nonpolar (hydrophobic), while NCC is highly polar (hydrophilic) thus leading to compatibility problems.[4–6] To improve compatibility between NCC and nonpolar polymers, different methods such as surface modification,[7,8] polymer grafting,[5,9] surfactants,[4,10] and coupling agents[11,12] have been studied. Although some studies on PP-NCC nanocomposites can be found in the literature[4,8] none of them used extrusion (melt blending) to compound their materials. Extrusion of nanocomposites is very important since PP is most commonly processed and compounded via extrusion. Hence, studying the extrusion processed PP-NCC nanocomposites and optimizing the conditions will help to understand the processing of NCC in the polyolefin market. Furthermore, addition of coupling agents, which are copolymers having both polar and nonpolar functional groups, is the simplest method to improve dispersion and adhesion between two components as no additional setup apart from those generally used to process the resins are needed. Nevertheless, the selection of a coupling agent is almost never discussed in the literature beside optimization of its concentration.

For polyolefin-based composites, maleated polyolefins such as MAPP and MAPE are now typical molecules used for different reinforcements such as glass fibers,[13] nanoclays,[14,15] and wood fibers.[16,17] Therefore, they are good candidates for NCC based nanocomposites. However, the main challenges are to find the best product available and to optimize the processing conditions to get the highest level of coupling between both phases leading to improved mechanical properties. In this context the most important parameters are the amount of maleic anhydride which determines the strength of the coupling agent/reinforcement adhesion, as well as the molecular weight of the coupling agent which is important for good interactions (entanglements) with the molecules of the bulk polymer. Finally, the ratio of coupling agent to reinforcement will influence both coupling efficiency (complete surface coverage) and cost issues as the price of MAPP (3–5 US$/kg) is higher than PP (1.5–2 US$/kg). Therefore the main objective of this work is to determine the optimum conditions (composition and processing) to obtain the best properties of the resulting composites. To achieve this

Table I. Characteristics of the MAPP Used in This Work

Code	MAPP	Supplier	Mw (kg/mol)	Acid value[a] (mg KOH/g)
A	Epolene E 43	Westlake Chemicals	9.0	45
B	Licomont AR405	Clariant	15.0	41
C	Eastman G 3015	Eastman	51.5	15
D	Eastman G 3003	Eastman	58.7	8
E	Orevac 18732	Orevac	208.2	2

[a] The values are taken from the data provided by the manufacturers.

objective, five different grades of MAPP having different molecular weight and acid value (AV) are used with different NCC : MAPP ratio. To compare the resulting materials, a detailed analysis of the mechanical properties (solid state) is presented and completed by rheological analysis (melt state), as well as physical and thermal properties.

EXPERIMENTAL

Materials and Sample Preparation

Polypropylene (PP) was used as the matrix: Profax 6323 from Basell having a MFI of 12 g/10 min (230°C/2.16 kg), a density of 0.90 g/cm^3 (23°C) and an Mw of 200 kg/mol. NCC was produced by acid hydrolysis of a commercial bleached softwood Kraft pulp according to a procedure reported elsewhere.[18] The resulting NCCs are crystals with an average length of 100–200 nm and a diameter of around 10 nm. Five different commercial grades of MAPP having different molecular weights and acid values (see Table I) were used as coupling agents. Before blending, all the materials were dried overnight at 60°C. To prepare the nanocomposites, first a concentrated masterbatch having 5 wt % of NCC was prepared in a twin-screw extruder (HAAKE Rheomex PTW 24 OS from Thermo Scientific, diameter = 16 mm, L/D ±25) with a flow rate of 0.5 kg/h. First, PP and MAPP pellets were dry-blended together and put in a feeder. Since NCC was in a dried form (powder) it was fed into the extruder by a special feeder designed for powder feeding. Before feeding the materials (PP and MAPP from one feeder and NCC from the other feeder), depending on the total feeding rate (0.5 kg/h) and the formulation, the feeding rate for each feeder was adjusted. Then, the masterbatch was diluted in a second extrusion step to achieve a final NCC concentration of 1 wt % with different filler/coupler (F/C) ratios: 1/2, 2/1, 5/1, 7.5/1, 10.1. These ratios were used as the sample coding in the manuscript. After some preliminary tests, the extruder temperature profile was set at 170, 180, 180, 180, 180, and 185°C from the feed zone to the circular die having a diameter of 1.73 mm. The compounds were pelletized to be later compression molded in a rectangular mold having dimensions of 100 × 100 × 2 mm^3. The samples were preheated at 190°C for 3 min and then kept at this temperature for another 3 min under a load of 2300 kg. The mold was then cooled down to 30°C under the same force. Finally, the samples for testing were directly cut in the molded plates.

Thermal Analysis

The thermal behavior of the samples was studied via differential scanning calorimetry (DSC) and thermogravimetric analysis (TGA). DSC was performed using a Perkin Elmer model DSC 7. Each sample was heated from 30 to 200°C with a heating rate of 10°C/min under a nitrogen atmosphere. TGA was performed on a Q5000 IR (TA Instruments) at a heating rate of 10°C/min from 30 to 700°C. The tests were performed in nitrogen and air atmospheres to evaluate both thermal and oxidative resistance of the samples.

Mechanical Properties

Tensile testing was performed at room temperature on an Instron model 5565 with type V samples having thickness of around 2 mm according to ASTM D638. The crosshead speed was 10 mm/min with a 500 N load cell. For each sample, testing was performed at least five times and the average result was obtained and reported with standard deviation. For flexural testing, samples with dimensions of 70 × 12 × 2.0 mm^3 were also cut in the compression molded plates according to ASTM D790. Flexural tests (60 mm span) were conducted using a crosshead speed of 10 mm/min on an Instron model 5565 with a 500 N load cell at room temperature. Each composition was tested with a minimum of five specimens to get an average and standard deviation for flexural modulus.

For notched Charpy impact test, rectangular specimens (110 × 12 × 2.0 mm^3) were cut from the molded plates according to ASTM D6110. The samples were then notched with an automatic sample notcher Dynisco model ASN 120m. For each composition, five samples were tested on a Tinius Olsen model Impact 104 to get the average and standard deviation for impact strength.

Rheological Measurements

Shear transient tests were performed on a strain-controlled TA Instruments rheometer (ARES) with a torque transducer (0.02–2000 g cm) and a normal force transducer (2–2000 g) under a nitrogen (N_2) atmosphere. The measurements were done using a 25 mm diameter parallel plate geometry with gaps between 1 and 1.5 mm at 180°C. Gap independence for such range has been presented elsewhere.[19] In the shear transient tests the shear growth functions were obtained at 180°C with a shear rate of 0.5/s. For large amplitude oscillatory shear (LAOS), the tests were performed on an ARES G2 (TA Instruments) in a strain-controlled mode by conducting strain sweep experiments in the nonlinear regime at 180°C and different frequencies (0.5, 1, 3 Hz). The obtained stress was then converted from a time to a frequency domain using Fourier Transform (FT)-rheology.[20]

Contact Angle Measurements

The procedure for contact angle measurement was reported elsewhere.[19] Films of PP and NCC were prepared for

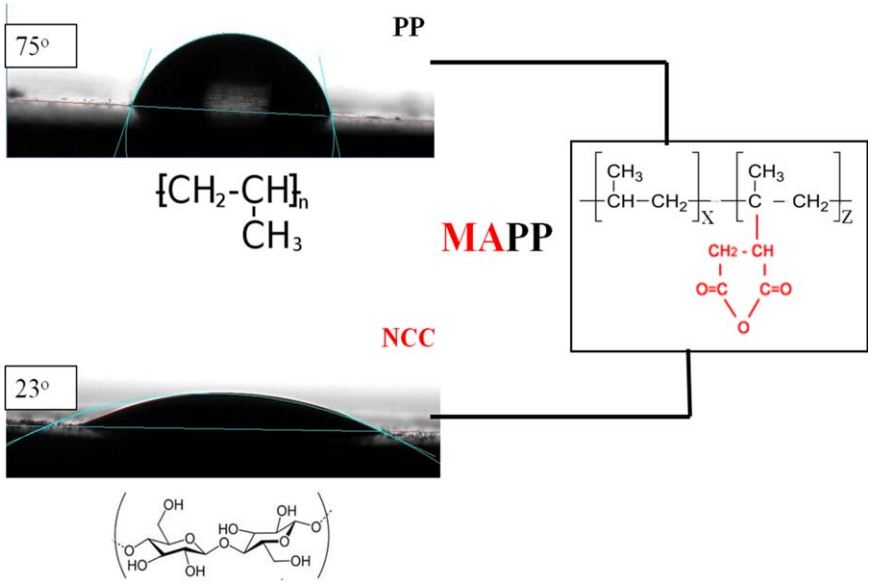

Figure 1. Water contact angle measurements for PP and NCC with schematic representations of their chemical structure. [Color figure can be viewed in the online issue, which is available at wileyonlinelibrary.com.]

measurements. For NCC, pills (0.5 g) with highly smooth surface were prepared by compression molding. As it can be seen in Figure 1, the surface roughness is very small compared to the size of the drop. An optical contact angle analyzer (OCA 15 EC Plus, Dataphysics) was used to measure the surface tension of PP and NCC. The system is composed of a high-resolution camera and a specific software developed to capture and analyze the contact angle on very small and curved surfaces. Small drops of 0.15 μL were dispensed via an ultrathin needle having an internal diameter of 0.18 mm.

Atomic Force Microscopy

A Nanoscope III Multimode AFM (Digital Instruments, Santa Barbara, CA), operated in the tapping mode, was used to capture images at ambient conditions. A J-scanner was used (maximum scan size 130 μm $\times$ 130 μm; min scan size 500 nm $\times$ 500 nm) with NSC15/AlBS silicon standard probes. The scan rates varied from 0.3 to 2.5 Hz depending on the scanned image size (from 100 μm $\times$ 100 μm down to 500 $\times$ 500 nm), the free oscillation amplitude was set to 2.0 V, and the amplitude set point was between 1.3 and 1.6 V.

RESULTS AND DISCUSSION

Surface and Thermal Properties

The results for water contact angle measurements of PP and NCC are shown in Figure 1 with a schematic representation of the chemical structure of both components. As mentioned in the "Introduction", PP has a nonpolar structure and therfore the water contact angle is high (75°) indicating its hydrophobic nature. On the other hand, NCC has several OH groups on its surface and is more hydrophilic which help the water drop to spread leading to a much lower contact angle (23°). The chemical structure of MAPP presented in Figure 1 shows that MAPP is composed of an apolar part (backbone) which has more affinity towards the bulk PP and a polar part (maleic anhydride part) which has more affinity towards NCC particles. Depending on the lenght of the backbone and the amount of maleic anhydride grafted (AV), the attraction toward each phase will be different and this issue will be discussed in the next sections. It should be mentioned that contact angle measurements for nanocomposites were also performed, but since the surface of the nanocomposites is covered mainly by a thin polymer film, the data were similar to neat PP.

Another important aspect of NCC based nanocomposites processing is thermal degradation. To determine the thermal stability of NCC, TGA measurements were performed and the results are presented in Figure 2. A first drop around 100°C can be associated with water molecules adsorbed on the particle surface. Although no water is believed to be absorbed inside NCC since the material is almost 100% crystalline, the high surface area due to the small sizes of NCC particles (length of around 100–200 nm, thickness of around 10 nm),[18] lead to an equilibrium moisture content of about 5%. Then, the main degradation starts at around 250°C. Since the processing temperatures were kept below 190°C, thermal degradation of NCC is believed to be negligible under these conditions as seen in the isotherm plot (less than 2% weight loss after 2 h).

Structure Analysis

It is known that due to the carbon based structure of NCC and polymer, both phases cannot be distinguished using typical microscopes such as TEM and SEM.[1,21,22] Nevertheless, optical images taken from films of the polymer and nanocomposites show that transparency is not significantly affected by NCC particles indicating that at least no large agglomerations are present in the system (see Figure 3). In order to get more insight into the nanocomposites structure, AFM was used and typical images are presented in Figure 3. It is clear that the appearance (texture) of PP and nanocomposite is different. The PP matrix seems more heterogeneous probably due to the presence of large crystallites giving an average roughness of 4.36 nm. On the

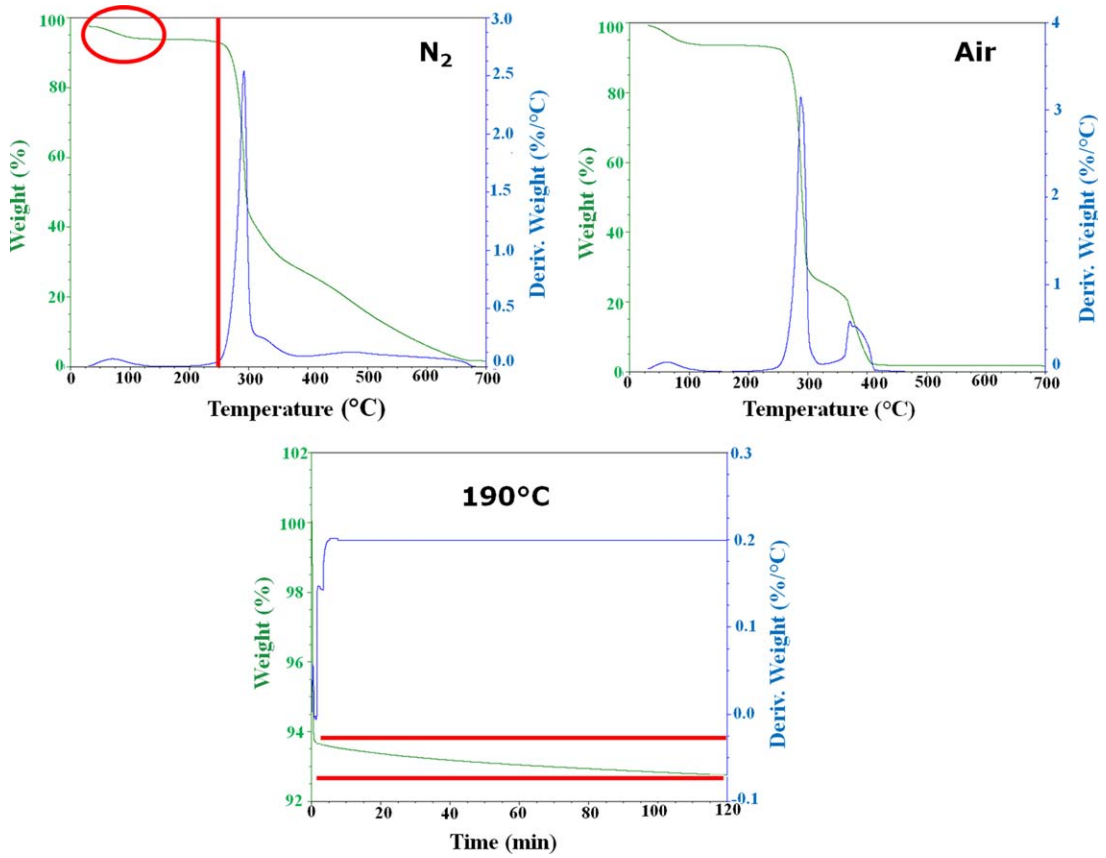

Figure 2. TGA results of NCC under different testing conditions. [Color figure can be viewed in the online issue, which is available at wileyonlinelibrary.com.]

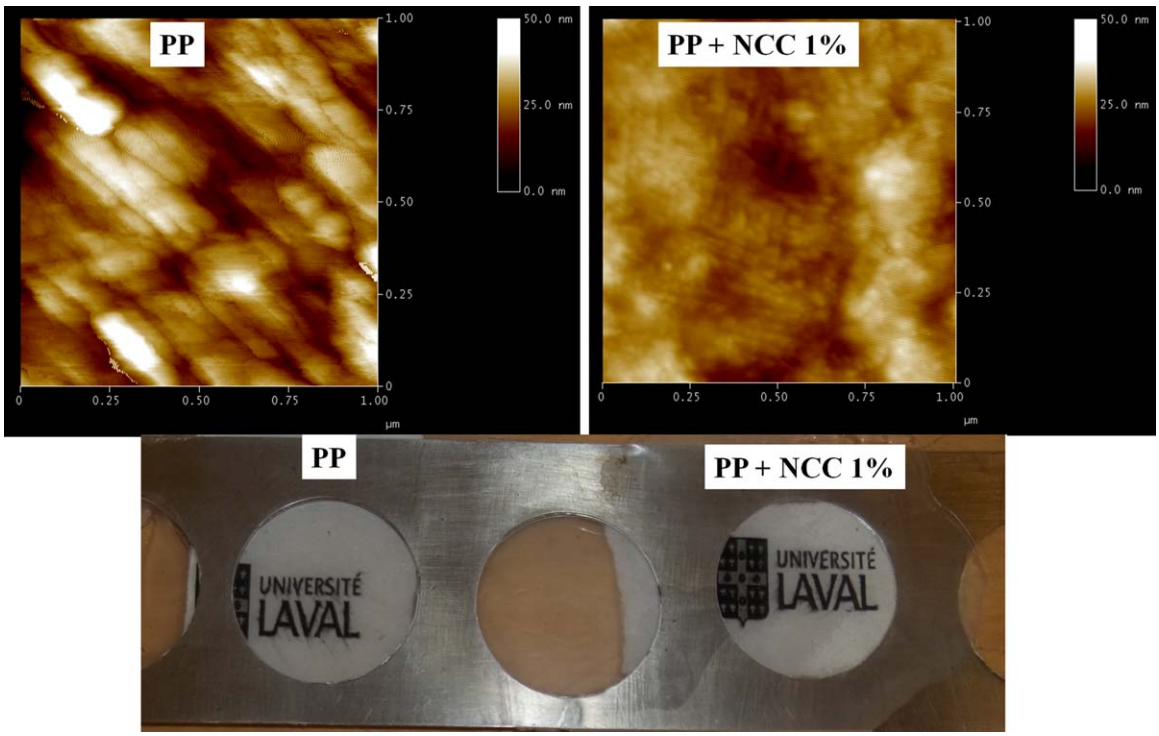

Figure 3. AFM images of PP and PP-NCC with 1 wt % (above) and optical images for the same samples (below). [Color figure can be viewed in the online issue, which is available at wileyonlinelibrary.com.]

Table II. Tensile Modulus for the Samples Produced with Different Filler/Coupler (*F/C*) Ratio

	F/C = 5/1		*F/C* = 7.5/1		*F/C* = 10/1	
Sample	Modulus (MPa)	Change compared to PP (%)	Modulus (MPa)	Change compared to PP (%)	Modulus (MPa)	Change compared to PP (%)
PP	450 (17)	-	450 (17)	-	450 (17)	-
PP NCC 1%	508 (10)	13	508 (10)	13	508 (10)	13
PP NCC 1% coupler A	584 (37)	29	599 (21)	33	565 (13)	26
PP NCC 1% coupler B	550 (18)	22	663 (50)	47	573 (32)	27
PP NCC 1% coupler C	495 (10)	10	556 (45)	24	519 (40)	15
PP NCC 1% coupler D	566 (27)	25	572 (50)	27	553 (38)	23
PP NCC 1% coupler E	509 (13)	13	574 (40)	28	528 (29)	17

Numbers in parentheses represent standard deviations. *F/C* is the filler/coupler ratio.

other hand, the addition of 1% NCC seems to produce a more homogeneous material probably due to the larger amount of smaller crystallites produced via heterogeneous nucleation at the particle-polymer interface. In this case, the presence of NCC particles reduced the value of the surface roughness to 1.69 nm. This hypothesis will be discussed later using thermal characterizations.

Mechanical Properties

Effect of Filler/Coupler (F/C) Ratio. The mechanical properties (tensile, flexural, and impact) of nanocomposites containing 1% NCC with different ratio of *F/C* are presented in Tables II–VI. It can be seen that, while the impact properties are not significantly influenced by NCC, flexural, and tensile properties changed considerably with the presence of NCC, as well as the filler/coupler (*F/C*) ratio, and nanocomposites with MAPP have better properties than without, showing the efficiency of the coupling agent used. However, it seems that regardless of Mw and AV, the optimum *F/C* ratio for all the coupling agents tested is around 7.5 : 1. Obviously, when the amount of MAPP is very low, there is a small amount of coupling sites available and it is not possible to completely connect the polymer and the available NCC particles. By increasing the amount of MAPP, more sites are available for coupling and the properties increase. However, when the particle surfaces are completely covered by MAPP, the addition of more MAPP molecules does not produce better adhesion and the extra MAPP molecules are dispersed in the bulk polymer acting as lubricant (plasticizers) leading to decreased mechanical properties at higher MAPP contents. This optimum content and its effect on mechanical performance have been reported several times for other systems.[23,24]

To verify the lubrication effect of extra MAPP, rheological measurements under shear transient were performed on samples having the smallest coupler (A) with very low *F/C* ratios (2/1 and 1/2) and the result are presented in Figure 4. The reason for this choice was that the smaller the molecule and the higher its amount, the higher is the lubrication effect.

In a shear transient test, the material flows due to chain disentanglement and sliding of chains (reptation)[25,26] and therefore the more difficult these phenomena the higher is the resulting stress.[19,27] Generally, in a stress–time curve after the first rise when the rate of entanglement and disentanglement become steady the stress reaches a steady state condition. For entangled materials in a shear transient test due to the possible chain stretching,[25] the stress goes through a maximum (stress overshoot) before decreasing to reach a steady condition. As seen in Figure 4, all the compositions here show such overshoot. However, the amount of overshoot is different. Adding MAPP produced lower stresses compared to neat PP indicating that

Table III. Tensile Strength for the Samples Produced with Different Filler/Coupler (*F/C*) Ratio

	F/C = 5/1		*F/C* = 7.5/1		*F/C* = 10/1	
Sample	Strength (MPa)	Change compared to PP (%)	Strength (MPa)	Change compared to PP (%)	Strength (MPa)	Change compared to PP (%)
PP	33.2 (0.7)	-	33.2 (0.7)	-	33.2 (0.7)	-
PP NCC 1%	32.3 (0.2)	−3	32.3 (0.2)	−3	32.3 (0.2)	−3
PP NCC 1% coupler A	39.1 (3.9)	18	40.2 (2.5)	21	36.5 (0.2)	9
PP NCC 1% coupler B	35.3 (2.1)	6	38.2 (3)	15	36.4 (1.2)	9
PP NCC 1% coupler C	35.7 (2.2)	6	38.1 (1.6)	15	36.2 (1.3)	9
PP NCC 1% coupler D	36.2 (1.5)	9	37.2 (0.8)	12	36.9 (0.7)	12
PP NCC 1% coupler E	33.8 (0.9)	3	37.3 (0.9)	12	36.1 (0.8)	9

Numbers in parentheses represent standard deviations. *F/C* is the filler/coupler ratio.

Table IV. Elongation at Break (%) for the Samples Produced with Different Filler/Coupler (*F*/*C*) Ratio

Sample	*F*/*C* = 5/1	*F*/*C* = 7.5/1	*F*/*C* = 10/1
PP	40 (5)	40 (5)	40 (5)
PP NCC 1%	30 (6)	30 (6)	30 (6)
PP NCC 1% coupler A	36 (2)	35 (8)	33 (2)
PP NCC 1% coupler B	39 (6)	38 (7)	37(4)
PP NCC 1% coupler C	33(5)	38 (4)	36 (6)
PP NCC 1% coupler D	37 (1)	40 (6)	39 (5)
PP NCC 1% coupler E	43 (9)	46 (7)	37 (2)

Numbers in parentheses represent standard deviations. *F*/*C* is the filler/coupler ratio.

MAPP facilitated chain disentanglement and/or sliding motion of the chains (lubrication). The addition of NCC increased the stresses compared to the sample having only MAPP. This can be related to the frictional forces and/or the attachment of macromolecular chains to particle surfaces reducing chain mobility.[28,29] Finally, when the amount of MAPP is very high (*F*/*C* = 1/2), the extra MAPP molecules are helping chain sliding under the applied shear leading to lower stresses. This is why an optimum MAPP content must be used in order to optimize properties enhancement while minimizing raw material costs.

The properties at break (tensile elongation at break in Table IV and impact strength in Table VI) did not change significantly with NCC addition showing that relatively good dispersion and coupling occurred for all the compositions as normally these properties decrease substantially with the addition of rigid particles, especially without good compatibility between the phases[30,31] and/or when the particles are not properly dispersed.[32,33]

Effect of Acid Value and Mw. After determining the effect of *F*/*C* ratio on the mechanical properties, the other objective was to study the effect of MAPP structure (Mw, AV). Since with the current methods for MAPP production, it is not possible to increase molecular weight and acid value together[16] and increasing one would results in the reduction of the other, it is important to find the optimum condition. Considering that the best MAPP : NCC ratio is 1 : 7.5, this ratio was used to determine the effect of Mw and AV. The results in Figure 5 are presented in a relative way, i.e., the value of the nanocomposite divided by the value of the neat PP matrix. It is clear that the optimum condition is not the same for flexion and tension. This is most probably due to the different nature of deformation in tensile and flexion. However, in both cases when the acid value is low (less than 40 for tensile and less than 10 for flexural properties) the mechanical properties are low which indicates the importance of maleic anhydride content for better coupling. However, when the acid value is high enough (higher than 40 for tensile and higher than 10 for flexural properties) no further improvement is observed by increasing AV. This behavior represents a compromise between the effect of acid value and molecular weight. This is reasonable with respect to maleic anhydride content: it should be high enough to properly attach to the NCC surface, but on the other hand when the particle surface is covered by MAPP then the nonpolar part of MAPP should be long enough to properly entangle with the bulk polymer macromolecular chains. It has been shown that the more similar the size of the bulk polymer (Mw of PP used here is around 200 kg/mol) and the attached chain the better would be the attraction between the bulk and coupler tail.[34,35]

Considering all the data obtained, it is clear that both Mw and AV are important. However, it seems that from a "coupling" point of view, acid value is the main parameter as there is more possibility for one MAPP molecule to attach to different NCC particles, thus creating a nanoscale network. When the amount of reacting site (MAPP) is appropriate, then the length of the backbone (MAPP) becomes important as it determines the strength of these connections with the polymer matrix. Therefore, there is an optimum for these values (intermediate range of Mw and AV) which represents a balance between the possibility to create bonds with the particles (high AV) and the degree of interaction with the polymer matrix (high Mw) without sacrificing processing and molecules mobility in processing (low Mw).

Thermal and Rheological Properties

The thermal properties (DSC) of the different nanocomposites are shown in Table VII. The melting point (T_m) and enthalpy

Table V. Flexural Modulus for the Samples Produced with Different Filler/Coupler (*F*/*C*) Ratio

	F/*C* = 5/1		*F*/*C* = 7.5/1		*F*/*C* = 10/1	
Sample	Modulus (MPa)	Change compared to PP (%)	Modulus (MPa)	Change compared to PP (%)	Modulus (MPa)	Change compared to PP (%)
PP	1711 (72)	-	1711 (72)	-	1711 (72)	-
PP NCC 1%	1809 (83)	6	1809 (83)	6	1809 (83)	6
PP NCC 1% coupler A	2011 (77)	18	2177 (30)	27	2021 (136)	18
PP NCC 1% coupler B	1970 (96)	15	2170 (83)	27	2000 (75)	17
PP NCC 1% coupler C	2188 (194)	28	2238 (165)	31	2084 (104)	22
PP NCC 1% coupler D	2195 (195)	28	2221(97)	30	1987 (137)	16
PP NCC 1% coupler E	1901 (30)	11	2041 (78)	19	2011 (91)	17

Numbers in parentheses represent standard deviations. *F*/*C* is the filler/coupler ratio.

Table VI. Impact Strength (kJ/m^2) for the Samples Produced with Different Filler/Coupler (*F*/*C*) Ratio

Sample	*F*/*C* = 5/1	*F*/*C* = 7.5/1	*F*/*C* = 10/1
PP	3.6 (0.16)	3.6 (0.16)	3.6 (0.16)
PP NCC 1%	3.0 (0.14)	3.0 (0.14)	3.0 (0.14)
PP NCC 1% coupler A	3.0 (0.17)	3.2 (0.13)	3.5 (0.14)
PP NCC 1% coupler B	3.3 (0.12)	3.5 (0.18)	3.5 (0.15)
PP NCC 1% coupler C	3.2 (0.16)	3.3 (0.17)	3.3 (0.18)
PP NCC 1% coupler D	3.4 (0.17)	3.4 (0.12)	3.2 (0.16)
PP NCC 1% coupler E	3.2 (0.14)	3.5 (0.19)	3.5 (0.18)

Numbers in parentheses represent standard deviations. *F*/*C* is the filler/coupler ratio.

(ΔH_m) are slightly reduced for all composites indicating that the size of PP crystals are reduced by NCC particles.[36] This is most probably due to NCC particles acting as nucleating agents for crystallization as such effect has been reported for cellulosic nanoparticles.[4,5,37] The higher the number of crystals, the smaller would be their size and since smaller crystals are easier to melt[36] and therefore lower ΔH_m and T_m is obtained for the nanocomposites. In the AFM images (Figure 3) small crystallite sizes in presence of NCC resulted in the appearance of a more homogenous surface for composites (roughness = 1.69 nm) than neat PP (roughness = 4.36 nm). However, since the differences in the thermal properties are not significant between the polymer and the nanocomposites these small changes might not

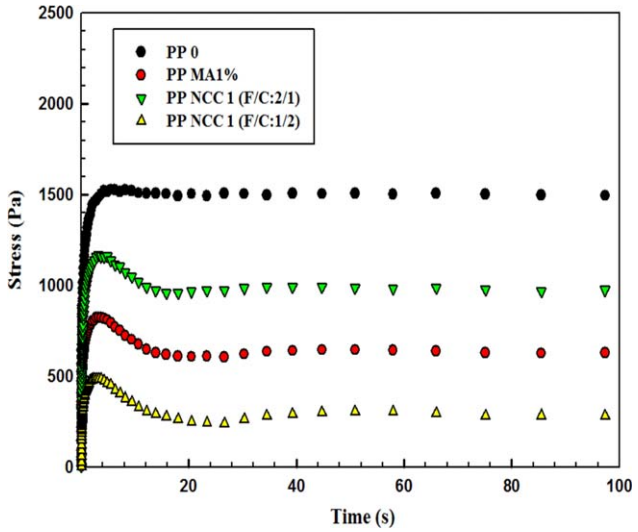

Figure 4. Step shear transient data for neat PP, PP MA1%, and PP NCC composites having different *F*/*C* ratios (2/1 and 1/2) for coupler A. [Color figure can be viewed in the online issue, which is available at wileyonlinelibrary.com.]

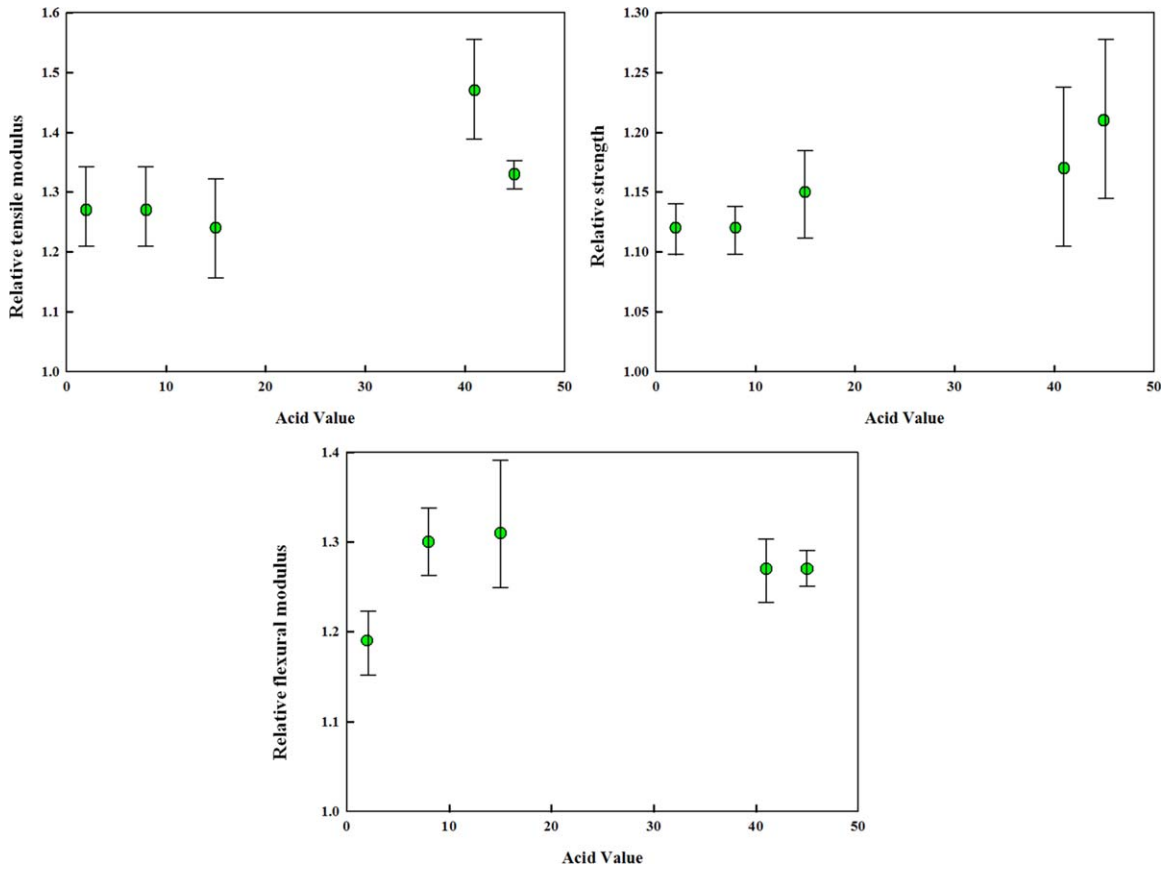

Figure 5. Relative mechanical properties of the nanocomposites for 1 wt % NCC with *F*/*C* = 7.5/1 to determine the effect of MAPP acid value and molecular weight. [Color figure can be viewed in the online issue, which is available at wileyonlinelibrary.com.]

Table VII. DSC Results of the Samples Produced

	F/C = 5/1		F/C = 7.5/1		F/C = 10/1	
Sample	ΔH_m (J/g)	T_m (°C)	ΔH_m (J/g)	T_m (°C)	ΔH_m (J/g)	T_m (°C)
PP	57.4	164.9	57.4	164.9	57.4	164.9
PP NCC 1% coupler A	55.6	162.8	56.6	163.3	56.7	162.8
PP NCC 1% coupler B	56.9	162.8	56.7	163.0	56.0	162.8
PP NCC 1% coupler C	56.5	163.0	56.0	162.1	55.9	162.8
PP NCC 1% coupler D	56.4	162.0	55.8	163.8	57.1	163.6
PP NCC 1% coupler E	57.3	164.1	56.7	163.4	56.4	163.8

F/C is the filler/coupler ratio.

significantly affect the mechanical properties (Tables II–VI). So crystallinity difference cannot explain the differences observed. It is important to note that the mechanical properties of the nanocomposite without coupling agent are lower compared to values with MAPP (see Tables II–V), while the thermal behavior for these two situations is similar. This is in agreement with our conclusion regarding the coupling effect of MAPP on the properties measured.

Another reinforcing mechanism which has been mentioned for nanoparticles is the formation of particle networks or percolation,[25,38–40] which can propagate the stresses. As mentioned in the morphological section, it is not possible to distinguish NCC particles from the polymer matrix by microscopic observations. Hence, it is not possible via image analysis to detect if a particle network (percolation) is formed or not. Considering the sensitivity of rheological properties to microstructure, rheology was used to investigate the structure. Since rheology is performed in the melt state, the overall polymer contribution in the composites is reduced compared to mechanical properties in the solid state. If particle concentration was high enough to create networks (percolation) then, due to the contribution of this solid network, there would be a large difference between the rheological properties of the neat polymer (matrix) and the nanocomposites. Looking at the melt rheological properties (Figure 6) it is clear that while the dynamic moduli of the nanocomposites are higher than for neat PP, the differences is much lower (orders of magnitude) than reported for percolated systems.[41,42] This means that the systems here are below the percolation threshold. The "under percolation" situation can be better verified by looking at the I_3/I_1 curve. One important manifestation of particle network formation in polymer systems is a large increase in the system nonlinearity, which can be studied via LAOS measurements. Under LAOS measurements, due to the contribution of nonlinear phenomena, the stress response shape is not sinusoidal like in SAOS measurements.[43] However, the distorted stress response is unique for each material and can be used to study the structure of complex systems. For this, the relative intensity of the third harmonic to the first harmonic (I_3/I_1) is used as a quantitative representation of the nonlinearity in viscoelastic materials.[25,43] In this context it has been recently shown that I_3/I_1 is a very sensitive parameter to detect structural changes close to the percolation concentration where a large increase in its value was reported when particles start to interconnect.[25] Looking at I_3/I_1 in Figure 6, it is seen that the value is almost the same for all the compositions indicating that the systems here is below the percolation concentration. Therefore, based on thermal and rheological results, it can be concluded that the observed mechanical

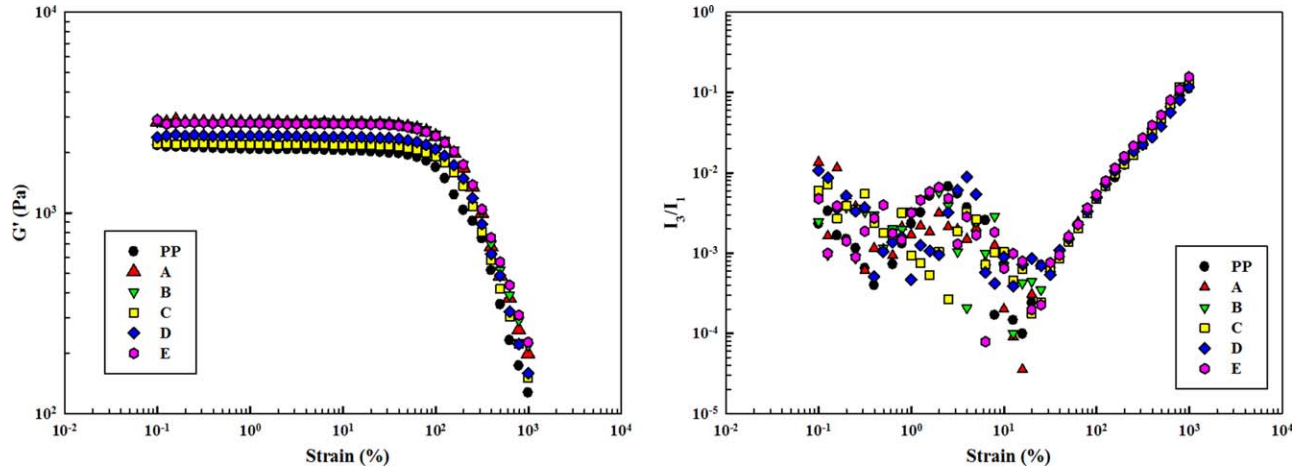

Figure 6. Storage modulus (left) and the nonlinear parameter I_3/I_1 (right) obtained under LAOS measurement for PP and PP NCC 1% with different couplers and a *F/C* ratio of 7.5/1 ($T = 180$°C and $\omega = 0.5$ Hz). [Color figure can be viewed in the online issue, which is available at wileyonlinelibrary.com.]

improvement is not related to crystallinity changes nor to the formation of particle networks, but it is mainly related to better interfacial adhesion (compatibility) between the polymer matrix (PP) and the reinforcing particles (NCC) which is resulting from the presence of coupling agent molecules.

CONCLUSION

In this work, melt blending (extrusion followed by compression molding) was used to produce polypropylene based nanocrystalline cellulose (PP-NCC) nanocomposites. In particular, five different commercial maleated polypropylene (MAPP) were used to determine the effect of molecular weight and acid number. From the samples produced mechanical properties (tensile, flexural and impact) were studied and completed with rheological and thermal properties.

The most important parameter was found to be the filler/coupler (*F*/*C*) ratio, but MAPP acid value and molecular weight have non-negligible effects. The first interesting finding was that regardless of maleic anhydride content and molecular weight, the optimum *F*/*C* ratio was the same for all the MAPP tested: 7.5/1. This optimum ratio seems to be related to the situation where the particle surface is completely covered by MAPP. At lower ratios the adhesion is not complete and when the particle surface is completely covered by MAPP, addition of more MAPP does not help coupling as extra MAPP molecules are not connected to the NCC surface but act as lubricant. The lubrication effect of extra MAPP was verified by analyzing the flow behavior of the samples where composites having very low *F*/*C* ratio (1/2) flowed under lower stresses compared to neat PP under a constant shear rate. The other two parameters (Mw and AV content) also are important, but from a "coupling" point of view, acid value is the most important since the first step in good coupling is that the coupler covers the particle surface and at high acid values there is more probability for MAPP molecules to attach to multiple reinforcing particles. For a fixed acid value, higher MW is better since the polymer tail can better interact with the bulk molecules. About these parameters even though one single coupler was not found to be the best for all the mechanical properties investigated here, the best mechanical properties were obtained for intermediate values. The highest tensile modulus improvement (47%) was found for coupler B (Mw = 15 kg/mol, AV = 41 mg KOH/g) and the highest flexural modulus (32%) was obtained with coupler C (Mw = 51 kg/mol AV = 15 mg KOH/g). The impact strength decreased slightly for all couplers except for coupler B where no significant change was observed.

Finally, thermal analysis showed lower PP melting temperature and melting enthalpy in the presence of NCC for almost all the composites indicates that crystal sizes are smaller. This seems to be confirmed by AFM analysis where surface roughness was decreased from 4.36 nm for the neat polymer to 1.69 nm for nanocomposites having 1% NCC. However, thermal property changes were not very significant to explain the large changes observed in mechanical properties. Also, analyzing the nonlinear behavior of the systems under LAOS measurements showed that the system is below percolation indicating that particle networks are not formed. Therefore, it can be concluded that the mechanical property improvement is mainly related to better adhesion between PP and NCC which is resulting from an optimized coupling systems in terms of MAPP content, molecular weight, and acid value, as well as processing (extrusion and compression molding) conditions.

ACKNOWLEDGMENTS

The authors acknowledge the financial support of NSERC (Natural Sciences and Engineering Research Council of Canada) and the Quebec Ministry for Economic Development, Innovation, and Exportation (MDEIE) for this work. Financial support from the Arboranano center of excellence was appreciated. Also, special thanks go to Jean Bouchard of FPInnovations for NCC samples. Finally, many thanks go to the group of Prof. Manfred Wilhelm at the Karlsruhe Institute of Technology (KIT) during a student exchange period sponsored by FQRNT (Fonds Québécois de la Recherche sur la Nature et les Technologies).

REFERENCES

1. Habibi, Y.; Lucia, L. A.; Rojas, O. J. *Chem. Rev.* **2010**, *110*, 3479.
2. Azizi Samir, M. A. S.; Alloin, F.; Dufresne, A. *Biomacromolecules* **2005**, *6*, 612.
3. Goffin, A. L.; Raquez, J. M.; Duquesne, E.; Siqueira, G.; Habibi, Y.; Dufresne, A.; Dubois, P. *Polymer* **2011**, *52*, 1532.
4. Ljungberg, N.; Cavaillé, J. Y.; Heux, L. *Polymer* **2006**, *47*, 6285.
5. Junior de Menezes, A.; Siqueira, G.; Curvelo, A. A. S.; Dufresne, A. *Polymer* **2009**, *50*, 4552.
6. Khoshkava, V.; Kamal, M. R. *Biomacromolecules* **2013**, *14*, 3155.
7. Fan, Y.; Saito, T.; Isogai, A. *Biomacromolecules* **2007**, *9*, 192.
8. Conzatti, L.; Giunco, F.; Stagnaro, P.; Patrucco, A.; Tonin, C.; Marano, C.; Rink, M.; Marsano, E. *Compos. A: Appl. Sci. Manufact.* **2014**, *61*, 51.
9. Araki, J.; Wada, M.; Kuga, S. *Langmuir* **2000**, *17*, 21.
10. Heux, L.; Chauve, G.; Bonini, C. *Langmuir* **2000**, *16*, 8210.
11. Ljungberg, N.; Bonini, C.; Bortolussi, F.; Boisson, C.; Heux, L.; Cavaillé, *Biomacromolecules* **2005**, *6*, 2732.
12. Xie, Y.; Hill, C. A. S.; Xiao, Z.; Militz, H.; Mai, C. *Compos. A: Appl. Sci. Manufact.* **2010**, *41*, 806.
13. Eberle, A. P. R.; Baird, D. G.; Wapperom, P. *Indus. Eng. Chem. Res.* **2008**, *47*, 3470.
14. Stoeffler, K.; Lafleur, P. G.; Perrin-Sarazin, F.; Bureau, M. N.; Denault, J. *Compos. A: Appl. Sci. Manufact.* **2011**, *42*, 916.
15. Koo, C. M.; Ham, H. T.; Kim, S. O.; Wang, K. H.; Chung, I. J.; Kim, D.-C.; Zin, W.-C. *Macromolecules* **2002**, *35*, 5116.
16. Keener, T. J.; Stuart, R. K.; Brown, T. K. *Compos. A: Appl. Sci. Manufact.* **2004**, *35*, 357.
17. Kim, J.; Pal, K. In Recent Advances in the Processing of Wood-Plastic Composites; Springer: Berlin, **2011**, Chap. 5.

18. Landry, V.; Alemdar, A.; Blanchet, P. *For. Prod. J.* **2011**, *61*, 104.
19. Hassanabadi, H.; Rodrigue, D. *Rheol. Acta* **2012**, *51*, 991.
20. Wilhelm, M. *Macromol. Mater. Eng.* **2002**, *287*, 83.
21. Tanem, B. S.; Kvien, I.; van Helvoort, A. T. J.; Oksman, K. In Cellulose Nanocomposites; American Chemical Society: Washington, DC, **2006**, Chap. 5.
22. Mahi, H.; Rodrigue, D. *Rheol. Acta* **2012**, *51*, 127.
23. Mechraoui, A.; Riedl, B.; Rodrigue, D. *Compos. Interfaces* **2007**, *14*, 837.
24. Gosselin, R.; Rodrigue, D.; Riedl, B. *J. Thermoplast. Compos. Mater.* **2006**, *19*, 639.
25. Hassanabadi, H. M.; Abbasi, M.; Wilhelm, M.; Rodrigue, D. *J. Rheol.* **2013**, *57*, 881.
26. Doi, M.; Edwards, S. F. The Theory of Polymer Dynamics; Clarendon Press: New York, **1989**.
27. Letwimolnun, W.; Vergnes, B.; Ausias, G.; Carreau, P. J. *J. Non-Newtonian Fluid Mech.* **2007**, *141*, 167.
28. Sarvestani, A. S. *Eur. Polym. J.* **2008**, *44*, 263.
29. Picu, R. C.; Rakshit, A. *J. Chem. Phys.* **2007**, *126*, 144909.
30. Kim, H.; Macosko, C. W. *Macromolecules* **2008**, *41*, 3317.
31. Tseng, C.-H.; Hsueh, H.-B.; Chen, C.-Y. *Compos. Sci. Technol.* **2007**, *67*, 2350.
32. Wakabayashi, K.; Pierre, C.; Dikin, D. A.; Ruoff, R. S.; Ramanathan, T.; Brinson, L. C.; Torkelson, J. M. *Macromolecules* **2008**, *41*, 1905.
33. Uddin, M. F.; Sun, C. T. *Compos. Sci. Technol.* **2010**, *70*, 223.
34. Srivastava, S.; Agarwal, P.; Archer, L. A. *Langmuir* **2012**, *28*, 6276.
35. Kumar, S. K.; Jouault, N.; Benicewicz, B.; Neely, T. *Macromolecules* **2013**, *46*, 3199.
36. Jiang, Q.; Yang, C. C.; Li, J. C. *Macromol. Theory Simulat.* **2003**, *12*, 57.
37. Ramires, E. C.; Dufresne, A. In Advances in Polymer Nanocomposites; Gao, F. Ed.; Woodhead Publishing: Cambridge, UK, **2012**.
38. Baxter, S. C.; Robinson, C. T. *Compos. Sci. Technol.* **2011**, *71*, 1273.
39. Scotti, R.; Conzatti, L.; D'Arienzo, M.; Di Credico, B.; Giannini, L.; Hanel, T.; Stagnaro, P.; Susanna, A.; Tadiello, L.; Morazzoni, F. *Polymer* **2014**, *55*, 1497.
40. Schlea, M. R.; Meree, C. E.; Gerhardt, R. A.; Mintz, E. A.; Shofner, M. L. *Polymer* **2012**, *53*, 1020.
41. Heinrich, G.; Klüppel, M.; Vilgis, T. A. *Curr. Opin. Solid State Mater. Sci.* **2002**, *6*, 195.
42. Cassagnau, P. *Polymer* **2008**, *49*, 2183.
43. Hyun, K.; Wilhelm, M.; Klein, C. O.; Cho, K. S.; Nam, J. G.; Ahn, K. H.; Lee, S. J.; Ewoldt, R. H.; McKinley, G. H. *Prog. Polym. Sci.* **2011**, *36*, 1697.